PFC/JA-96-12

Neutral Particle Dynamics in the Alcator C-Mod Tokamak

A. Niemczewski, I.H. Hutchinson,
B. LaBombard, B. Lipschultz, G.M. McCracken

May, 1996

Submitted to Nuclear Fusion.

This work was supported by the U. S. Department of Energy Contract No. DE-AC02-78ET51013. Reproduction, translation, publication, use and disposal, in whole or in part by or for the United States government is permitted.

NEUTRAL PARTICLE DYNAMICS IN THE ALCATOR C-MOD TOKAMAK

A. Niemczewski, I. H. Hutchinson, B. LaBombard, B. Lipschultz, G. M. McCracken

Plasma Fusion Center
Massachusetts Institute of Technology
Cambridge, MA 02139

ABSTRACT

An experimental study of neutral particle dynamics has been carried out over a wide range of operating conditions in Alcator C-Mod using special-purpose pressure gauges. Both divertor and mid-plane pressures are found to depend primarily on the edge plasma regimes defined by the scrape-off-layer heat transport. While the maximum divertor neutral pressure (30-60 mTorr) is achieved at high core plasma densities ($\bar{n}_e$=2 - 4x10^{20} m^{-3}), corresponding to the detached divertor state, the maximum ratio of divertor to mid-plane pressure (~70) is achieved in the high-recycling transport regime. Variations in the divertor geometry have a weaker effect on the neutral pressures. For otherwise similar plasmas the divertor pressure and compression are maximized when the strike point is located at the bottom of the vertical target plate. Modelling shows that the high pressure sustained during detached divertor operation (despite a considerable drop in the recycling source) can be explained by scattering of neutrals off the cold plasma plugging the divertor throat.

1 Introduction

The neutral pressure in the tokamak boundary has been studied for many years. In early measurements with limiter tokamaks it was noted that the pressure dropped rapidly as the plasma formed due to the high effective pumping speed of the plasma. [1] When divertors were developed it was observed that the neutral pressure in the divertor private flux region was considerably higher than that near the confined plasma.[2,3]. It was recognized that this compression might be advantageous for pumping the plasma and in particular for pumping the helium ash from fusion reactions. A number of studies have investigated the compression of helium in the divertor.[4,5] It was found that physically restricting the conductance between the divertor region and the main chamber enabled the compression ratio to be increased and compression ratios of 10 to 20 were typically found for hydrogen and deuterium in PDX [6,7], while compressions up to 300 were obtained in Doublet III [3], and divertor pressures up to 1mbar were obtained in ASDEX [2,8]. Evidence of a low temperature (< 5eV) divertor plasma was found [2,3,7] and it was pointed out that at these temperatures the charge exchange rate greatly exceeded the ionization rate, which might result in a high probability of atom backscattering from the plasma[4,7]. Most of the physical picture described in the early reviews [2,8] has been substantiated by subsequent studies.

More recently the mechanism of detachment of plasma from the divertor target has been discussed and the loss of momentum by ion-neutral collisions proposed.[9,10] Detachment can be defined as the loss of pressure along a field line so that not only can there be density and temperature gradients but also pressure gradients between the core plasma and the divertor target. Detachment results in the reduction of both power and particle flux at the target and may be a useful technique for reducing the the peak power density in ITER [11]. One of the motivations of the present study is to measure the neutral density in the divertor region to see under what conditions it is high enough to account for detachment. Moreover there is evidence that low neutral density surrounding the core plasma correlates with high core confinement [12] so that there is motivation for achieving good compression ratios between the divertor and the core plasma. An overview of neutral plasma interactions has been presented by Heifetz [13] and much of the relevant atomic physics has been discussed by Harrison [14]. In this paper we report a study of neutral pressure both in the divertor and at the mid-plane of

the Alcator C-Mod tokamak under a range of operating conditions. These include a wide range of plasma densities, varying plasma currents, geometry and reversal of the BxVB ion drift. We have looked in particular at the neutral compression, defined as the ratio of divertor private flux zone to mid-plane neutral pressures.

2 Experiment

Alcator C-Mod [15], has the attractive characteristics of high operating density, due to high magnetic field, and a geometrically closed divertor, allowing high neutral pressures to be achieved. Operating parameters are R =0.67 m, a =0.21 m, B_t =5.3 T, I_p =0.6 to 1.0 MA, n_e=0.5 to 2.5x10^{20} m^{-3}. The primary diagnostic used in the present experiments is a set of neutral pressure gauges, which include standard Bayard-Alpert (B-A) [16] and capacitance gauges, and fast linear-ionization gauges [17], based on the ASDEX gauge principle [18,19]. Fig. 1 shows the location of the pressure gauges inside the tokamak and the main neutral particle reservoirs of interest. The two fast linear ionization gauges (MIT gauges), built for high-noise, high magnetic field operation, were used in the present experiments , one in the gas-box reservoir and one in a similar poloidal position but at a toroidal position where the gas box is open to the Scrape-Off Layer (SOL), the common flux zone.(fig. 1). The MIT gauges were subjected to extensive calibration experiments with on-axis toroidal fields up to 5.3 Tesla and vertical fields up to 0.6 Tesla,. The gauge sensitivity increases monotonically with B_t being approximately linear between 1 and 5.3 Tesla [17] and having a maximum sensitivity 11 times the value with no field. The effect of the vertical field on gauge sensitivity is small during steady state operation, but time varying fields produced significant perturbations[20]. All measurements presented have been taken with constant magnetic fields. The time response of the gauge is typically 2 ms, but the response time of the volume and conductance considered is ~ 6 ms.

The B-A gauges and the capacitance gauges are used in positions further from the plasma in regions of lower magnetic field (0.02 -0.2 Tesla) and therefore have a slower time response. They are magnetically shielded and were adequate for making measurements in steady state plasma conditions. The B-A gauge is used primarily for the low pressure measurements at the mid-plane. This gauge has a time constant of ~17 ms for D_2. The capacitance gauges were MKS baratrons [21] which have an absolute accuracy of better than 5%. These gauges were used both for *in situ* calibration of the

MIT and B-A gauges and for real time measurements. They typically had a time response of ~30 ms.

The other parameters of direct importance to the interpretation of the neutral pressures are the ion fluxes to the divertor target and the plasma electron temperature and density, T_e and n_e, in the SOL. These are measured by an array of probes on the inner and outer divertor targets and a scanning probe which measures the upstream values of the T_e and n_e profiles, approximately 5 to 10 m from the target along a field line, fig. 1 [22]. There are three probes at each poloidal position on the divertor target; two are flush with the tile surface and one has a "domed" end protruding from the surface. The domed probes have a well defined surface area projected parallel to the magnetic field lines and when operated with a swept bias voltage allow the plasma T_e and n_e and floating potential V_f to be determined. One of the flush probes at each poloidal position is operated at a fixed negative bias and is used for measuring the time dependence of the ion saturation current to the target as discussed in section 3. The upstream SOL profiles of the plasma T_e and n_e are measured with a fast scanning probe which can be inserted up to 3 times per discharge [22]. Although there are four separate tips on the scanning probe head the results are averaged for the purposes of the present study.

3 Results

3.1 Time dependence of neutral pressures

Fig. 2a shows the time history of the neutral pressure in the divertor and the mid-plane in a high density Alcator C-Mod discharge. A strong deuterium gas injection into the divertor region between t =0.55-0.7 sec. causes the core plasma density (trace #2) to increase by about a factor of three, but the divertor neutral pressure (trace #3), to increase by about a factor of one hundred. Detachment starts at ~0.58 s. While the 60 mTorr divertor pressure remains constant until the end of the discharge (disruption at t=1.02 sec.), the mid-plane pressure (trace #4) gradually increases, resulting in a decreasing divertor-to-mid-plane pressure ratio (trace #5).

The detailed temporal behavior of the ion current to the target and the neutral pressures during detachment are shown in fig 2b. A fast divertor detachment, due to

neon injection, occurs at t=0.86 sec. (as indicated by the ion saturation current signature - traces #1 and #2), with re-attachment occurring at t=0.94 sec. The current to probe 4, which is on the vertical plate, drops significantly while the current to probe 8, which is above the nose, rises slightly. Trace #4 depicts the open-module and trace #5 (suppressed zero) the closed module divertor pressures. The closed divertor module pressure drops at detachment and at reattachment returns to its initial value. In contrast, the open divertor module pressure (trace #4) increases as a result of detachment and drops as a result of reattachment. The "fast" detachment shown in fig 2b typically results from impurity injection, either a spontaneous or a deliberate injection. With low impurity levels detachment generally occurs more gradually, with the ion current to the target decreasing smoothly over ~ 100 ms as the density is raised through the critical detachment value.

The closed divertor module neutral pressure is measured in a "gas box" volume, connected to the plasma private flux zone. It is therefore not sensitive to the horizontal target plate recycling but only to that on the vertical plate. At detachment the integrated ion current to the vertical plate drops typically by a factor of 4 while the pressure drops only by about 20%. Both divertor ion current and neutral pressures revert to their original values at reattachment. This dependence is analyzed quantitatively in section 4. The time history of the H_α radiation correlates with the open divertor module pressure observations. The H_α signal is from a detector viewing the outer divertor and is a measure of the recycling flux above the outer diverter nose. A quantitative analysis of the open divertor module pressure is difficult because of an intrinsic three-dimensionality of the problem (lack of toroidal symmetry) and is not attempted here.

Fig. 2b shows also the mid-plane neutral pressure (trace #6). There is no sudden change in the mid-plane pressure at detachment, but rather a faster rate of rise. This behavior can be explained by increased recycling on the horizontal shelf. As a result of the mid-plane pressure rise, the divertor compression (p_{div}/p_{mid}) continues to drop throughout the detached state; it recovers, however, to its pre-detachment value after reattachment (trace #7 on fig. 2b).

3.2 Parametric dependence of neutral pressures

(a) SOL transport regimes.

Fig. 3a shows the mid-plane pressure plotted as a function of line averaged core plasma density. The pressure increases monotonically with density but the rate of increase is larger at higher density. Fig. 3b shows the scaling of the divertor neutral pressure with the core plasma density. The divertor pressure is low at low n_e, increases approximately linearly at intermediate density, then increases more slowly at high density. The pressure continues to increase at higher density even in the detached regime, as has been seen on DIIID [23] and JET [24]. The general behavior with density is closely correlated with the sheath limited, conduction limited [25] and detached regimes in the SOL and divertor. These regimes have been experimentally characterized in Alcator C-Mod by LaBombard [22]. At low density ($\bar{n}_e$=0.5x10^{20} m^{-3}, I_p =800 kA) there is little temperature gradient along the field lines between the mid-plane and the target, the temperature drop being all at the plasma sheath. In this "sheath-limited" regime the mid-plane and divertor neutral pressures are both low (p_{mid}=0.05 mTorr, p_{div}=0.5 mTorr). At higher density there is a conduction limited transport regime where pressure balance along the field lines is maintained, but there is a significant temperature gradient along the field lines leading to high recycling near the target plates [25]. At very high density the detached divertor regime is obtained where pressure is no longer constant along the field lines [22, 26]. Here p_{mid} =1-4 mTorr, and p_{div} =30-60 mTorr at n_e=2-4x10^{20} m^{-3}. The different regimes are shown by different symbols in fig. 3 to emphasize the correlation . The divertor-to-mid-plane neutral compression ratio, shown on fig. 4, is low (~10) in the sheath-limited regime, reaches the maximum (~70) in the high-recycling regime and decreases through the detached state. The decrease is due to the rapid rise in the mid-plane neutral pressure, which is correlated with the increase in the ion current to the target plate above the divertor nose – see section 3.3.

Fig. 5 illustrates the dependence of the compression ratio on the plasma current. For different plasma currents the divertor compression curves shift to lower or higher core densities, following the shift of the edge plasma transport regimes. A drop in the compression ratio at core densities about ~20% below the detachment threshold correlates with a decrease in the fraction of the ion flux on the vertical plates, with respect to the total divertor flux. These detachments occur relatively slowly, as discussed in section 3.1. Even in the case of fast detachments the ion current frequently decreases by a factor of 2 or more from its maximum value before the fast detachment occurs [27].

(b) Divertor Geometry

Variations in the divertor geometry have a much weaker effect (compared with the edge plasma characteristics) on the divertor pressure and compression ratio, causing less than a factor of two change. Fig. 6 shows the divertor pressure variation as the outer strike point is moved along the outer divertor plate. The effective divertor geometry is varied from flat plate target , with the strike point above the outer divertor nose, to vertical target , with the strike point below the nose and then to slot geometry, fig 1. The neutral pressure is maximized when the strike point is located at the bottom of the vertical target plate (i.e., the minimum distance between the gas-box entrance and the strike point). Similar results have been observed in DIIID [28-30] and JET[24, 31]. The results from DIII-D at high density [30] show less dependence on divertor geometry than the earlier data [28,29] and are in better agreement with our results. The divertor pressure when the strike point is on the outer divertor target above the nose, is similar to that measured in the vertical-plate configuration, whereas the compression is as much as a factor of two smaller (fig. 7). The higher midplane pressure is probably due to more of ion flux being above the nose, providing a larger source in the main chamber. Within the scatter of the experimental data the ion $B \times \nabla B$ drift direction has a negligible effect on the neutral compression ratio (and pressures), fig. 8, despite the fact that, at low density, inside/outside recycling asymmetries are observed [32].

3.3 Comparison of neutral pressure with target ion flux

It seems probable that the principal source for the neutral density in the divertor private flux zone and behind the outer divertor target is the flux of ions neutralized at the target surfaces. It is therefore interesting to compare the neutral density with this flux. Using the measurements from the probes in the target, the total ion flux has been integrated spatially over the target surface in two regions: on the inner and outer "vertical" sections below the nose and on the outer plate above the nose, see fig 1. Because of the geometry (fig. 1) it is expected that the flux to the target vertical sections will be the dominant contributor to the neutral density in the private flux zone and the flux to the outer plate above the nose will contribute to the neutral density in the main chamber.

For the present comparison we use the parallel ion flux density measured by the tile-mounted domed Langmuir probes multiplied by the sine of the field-line incidence angle, which is typically 0.5 -1.0° for the vertical sections. The use of the domed probe data however will be re-examined in section 4.2. Fig. 9a illustrates the mid-plane pressure

plotted against the outer divertor target flux to the horizontal sector and fig. 9b, the divertor neutral pressure plotted against the integrated ion flux to the vertical sections of the divertor plate. The mid-plane pressure is monotonic and almost linear with the ion flux, independent of the SOL plasma regime, fig. 9a. On the contrary the divertor pressure is double valued, being low in the sheath limited regime and high in the detached regime for equal values of ion flux to the target, fig. 9b. This suggests that the sink for neutrals in the divertor must be varying strongly between these two regimes.

4 Interpretation and modeling

4.1 Neutral particle flux model

A number of attempts have been made to model neutral transport in the divertor using Monte Carlo techniques[33-37]. In some cases good agreement with experiment has been reported. However in DIII-D [34] it was noted that the value of the divertor neutral pressure calculated from DEGAS was significantly below the experimental value. Divertor modelling of the C-Mod divertor using the DEGAS code [38] has been under way for some time, looking both at the neutral pressure and the H_α spatial distribution. It has been found that the neutral pressure is typically an order of magnitude below the experimental values and the spatial distribution of the H_α is narrower than the experimental data. It is possible that the Monte Carlo codes do not include all the neutral physics required for the high density conditions of C-Mod.

In view of the above and in order to obtain a quantitative interpretation of the divertor neutral pressure measurements across the experimental range of edge plasma parameters we propose a simple lumped model which balances the fluxes that fuel and deplete the divertor particle reservoir. This reservoir is taken to be the private flux zone (PFZ) and the volume behind the outer divertor structure. The fluxes are shown schematically in fig. 10. In steady state the divertor neutral flux balance equation can be written as:

$$0 = f_{tr} \cdot \Gamma_{plate} - (1\text{-}A)\ \Gamma_{kin} - \Gamma_{leak} \qquad (1)$$

The flux of neutrals entering the PFZ is $f_{tr}.\Gamma_{plate}$, where Γ_{plate} is the ion flux to the plate below the nose, and f_{tr} is the probability of transmission of the atoms neutralized at the target plate through the SOL. The flux of neutrals escaping from the PFZ is (1-A) Γ_{kin}

$+\Gamma_{leak}$, where Γ_{kin} is the gas kinetic flux of neutrals from the private flux zone back across the separatrix into the SOL, Γ_{leak} is the neutral flux escaping through the structure from the gas box into the main plasma chamber, and A is the average albedo of the plasma for the gas kinetic flux impinging on it.

We first consider the relative magnitudes of the neutral source resulting from the incident ion flux and the kinetic flux of neutrals impinging on the plasma surface, deduced from the neutral pressure, i.e., consider $A=\Gamma_{leak}=0$, $f_{tr}=1$. The ratio $\Gamma_{plate}/\Gamma_{kin}$ is plotted in fig. 11 as a function of plasma density; it varies over almost two orders of magnitude between low and high density cases. A possible explanation for the apparent particle imbalance as the density increases, is that atoms or molecules entering the plasma from the PFZ have a low probability of ionization and a high probability of scattering in the plasma (or reflection off the plate), Such an effect would be expected when the plasma density is high and the temperature is low. During detachment the measured T_e is less than 5 eV so that the probability of ion scattering greatly exceeds that of ionization.[39]

To make an estimate of the average albedo we consider the model of the plasma-neutral interaction shown in fig. 12 [20]. Ten separate chords are used, representing different neutral atom trajectories, and the albedo is calculated for each, using a 1-D approximation. For the shorter chords (#2-7 and #12) ending at the plate the neutral transmission probability is calculated based only on the probability of ionization and reflection from the target. This is because λ_{CX} is less than the distance from the separatrix to the target plate. In this case the albedo expresses the probability of an atom not being ionized upon crossing the plasma fan twice (with reflection from the plate). For the longer chords stretching across the divertor throat (#9-11) we use a diffusive transport approximation because the momentum-transfer mean-free-path (λ_{mt}) is much shorter than the path length [20]. The albedo is obtained from a numerical solution of the neutral diffusion equation. The ratio of the diffusive flux, Γ_D,to the incident flux Γ_{in} is

$$\Gamma_D/\Gamma_{in} = -D_n.\ \text{grad}\ N/\ 0.5\ v_o\ N$$

where D_n is the diffusion coefficient, v_o the thermal velocity and N the density. In the limit where the mean free path is small compared to the physical dimensions the approximation can be made

$$A = 1 - \Gamma_D/\Gamma_{in} = 1 - \lambda_{mt}/L_D \qquad (2)$$

where L_D is the thickness of a "diffusive" plasma zone, and where ionization is negligible compared to scattering (elastic or charge-exchange). Such a cold plasma region exists in a detached divertor. The final albedo needed in eq. 1 is obtained from a weighted average over the plasma boundary and expresses the probability of an escaping neutral reappearing in the PFZ-reservoir after scattering off the plasma or reflection off the plate.

In order to calculate the contributions of ionization and scattering we need to know T_e and n_e everywhere in the plasma, just as in the case for Monte Carlo calculations. From the probe data we have profile measurements of T_e and n_e both at the target plate and at a single poloidal position upstream on the flux surface. By using a conduction model, T_e and n_e at any point on the flux surface can in principle be obtained [22]. Two methods of performing this interpolation of the plasma parameters along a flux surface have been used . The details of these models are discussed in the Appendix. Ionization and charge exchange reaction rates are obtained from Janev [33] The rate coefficient for momentum transfer has been assumed to be equal to the charge exchange rate. In separate calculations we have used twice the charge exchange rate to estimate the effect of the uncertainty in the elastic scattering cross section [36, 41,42]. Particle reflection coefficients given by Thomas et al [43] are used to calculate the reflection of neutrals at the molybdenum target plate.

The components of the balance equation, eq. 1, have been evaluated for steady state discharges over a range of densities. The total perpendicular ion flux striking the vertical target plates (Γ_{plate}) is obtained from the domed divertor Langmuir probe measurements as in fig. 9b. After neutralization, particles cross the SOL into the private-flux-zone (PFZ) reservoir. The flux of neutrals escaping through leaks in the divertor structure (Γ_{leak}) is calculated from the gap conductance, the gas-box pressure and an estimate of pressure outside the divertor. The kinetic flux of neutrals crossing the neutral-reservoir/PFZ-plasma boundary (Γ_{kin}) is derived from the divertor pressure measurement as described above. Because of the remote location of the pressure gauge (fig. 10), the measured value has to be related to the neutral density in the divertor PFZ. If it is assumed that the atoms at the separatrix, near the boundary of the PFZ and the SOL, are heated to ~3eV by elastic collisions and molecular dissociation, then it can be shown that they must have a mean free path large compared to the divertor dimensions. We have therefore

assumed particle flux conservation to calculate the neutral flux at the separatrix from the measured value in the gas box.

Table 1 summarizes the values of the particle flux balance components, calculated for five representative discharges, spanning the sheath-limited, high-recycling, and detached-divertor regimes.

4.2 Model discussion and uncertainties

Taking the "constant T_e" plasma model described in the Appendix the source-to-sink ratio, plotted in fig. 13, varies by about a factor of two across the entire range of plasma parameters, indicating approximately constant particle balance. The ratio of the ion recycling source (Γ_{plate}) to the gas kinetic flux (Γ_{kin}) for the modeled discharges is also plotted in fig. 13 for comparison.

The fact that the value of the ratio of the source neutral flux ($f_{tr}\cdot\Gamma_{plate}$) to the sum of the losses(equation 1) is less than unity is probably due to an underestimate of the perpendicular ion flux from the domed probe data and to the uncertainty in the estimate of the neutral flux density in the PFZ. It is well known that it is difficult to interpret the results from probes which have an oblique angle < 2-3^o to the field lines [44,45] We have compared the results from the domed probes and the flush probes and found that for the vertical plate section, where the angle between the field line and the surface is typically 0.5° - 1.0°, the ratio of the flush to domed probe integrated ion currents is about 10 . For the plate section above the nose, where the angle between the field line and the surface is typically 2 - 4°, the ratio of the two currents is about a factor of 4. Over a wide range of densities the two values are approximately proportional to each other. It is expected that the current density to the flush probes will be an overestimate of the ion flux because the probes are biased, resulting in an extended sheath [46]. The current density from the domed probes on the other hand is expected to be an underestimate of the perpendicular flux since enhanced cross field diffusion induced by the presence of the surface is not accounted for [45]. This is particularly evident at high density (the detached plasma cases), where the neutral leakage flux alone ($\Gamma_{leak,}$), calculated from vacuum conductance and pressure measurements, is larger than the domed probe determination of the ion flux source ($f_{tr}\cdot\Gamma_{plate}$), (compare Table I). In this case particle balance cannot be obtained using the domed probe measurements for any value of the albedo.

With the "constant T_e" model the high divertor neutral pressure is sustained in the detached state, despite a considerable drop in the recycling source. This can be explained by the scattering of neutrals off the cold PFZ-plasma plugging the divertor throat and reflection off the target plates, provided the detachment front is well separated from the plates.

An identical set of calculations comparing source and sink, shown in fig. 13, has been carried out with the simple analytic electron-conduction plasma model discussed in the Appendix. The resulting plasma profiles have low T_e only very close to the plate ie the detachment front is close to and parallel to the plate. While this plasma model gives a result which is similar to that of the "constant Te" model at low density, it has too large a sink, i.e., too low an albedo at high density, table I. Thus the high albedo necessary to explain the data is only obtained if the plasma temperature is low over a large fraction of the separatrix in the PFZ. There are other reasons to believe that the position of the strong temperature gradient along the field is further from the target than predicted by the conduction model. For T_e high near the plate, additional ionization in the SOL would occur resulting in an ion flux to the target near the separatrix much in excess of what is observed during detached discharges. Moreover, the ionization and excitation of these neutrals would result in a hydrogen power loss in excess of the power crossing the separatrix. More detailed measurements of the plasma profile in the divertor and more detailed modeling are desirable to confirm our conclusions.

From Table I we see that neutral escape through the leaks in the divertor structure becomes a significant loss channel at high divertor pressures. In particular, in the detached divertor state the net loss of neutrals towards the plasma becomes smaller than the leakage. This leads us to believe that the neutral confinement in the Alcator C-Mod divertor can be significantly improved. Two modifications of the divertor have been considered – closing the leakage slot and widening the divertor throat to maximize recycling on the vertical target. Both modifications were predicted to produce an increase in the compression ratio of a factor of three to seven [20]. Subsequent experiments with the slot closed have resulted in an increase in the compression ratio of ~ 5.

5 Conclusions

The experiments described have extended earlier studies to much higher densities and shown that there is a strong dependence of the neutral pressure, both in the main plasma chamber and in the divertor, on the SOL conditions. Both regions show the neutral densities increasing monotonically with $\bar{n}_e$. However, while the highest divertor neutral density occurs with a detached divertor plasma the highest compression ratio of the divertor to mid-plane pressure occurs in the high recycling regime. The maximum compression ratio shifts to higher density with increasing plasma current.

The effect of geometry on the neutral density and the compression is less dramatic. The compression ratio is a maximum when the strike point is on the vertical target plate just above the entrance to the gas box and is minimized (about a factor of 2 lower) when the strike point is just above the divertor nose. No significant difference in neutral pressure is observed for fixed core plasma parameters when the $B \times \nabla B$ ion drift direction is reversed.

An increase in the divertor neutral pressure occurs as detachment progresses despite the fact the ion flux to the target below the divertor nose has dropped by typically a factor 4. This has led to the hypothesis that the albedo of the plasma for neutral atoms impinging on it from the private flux zone increases towards unity at high divertor plasma densities and low plasma temperatures. A simple global model of the neutral fluxes, taking into account ionization, plate reflection, and neutral-ion scattering supports this hypothesis, if certain assumptions about the plasma temperature gradient along field lines are made. The high albedos are consistent with two other observations; (i) that the gas kinetic flux of neutrals does not result in an excessive power loss and (ii) that the ion flux to the target at the strike point is often an order of magnitude lower than the value higher up the plate. (see appendix)

If operation can be achieved with the divertor plasma conditions close to those obtained in Alcator C-Mod, i.e., ionization and scattering mean-free-paths being much shorter that a typical escape distance, a narrow divertor throat is not critical since neutrals are confined in the divertor volume by the plasma plugging the throat itself. The increased neutral compression recently obtained by reducing the conductance from the divertor back to the main chamber confirms that in the experiments described the

main particle loss mechanism is through this conductance and that the plasma plugging at the divertor throat is very efficient.

Acknowledgments

We are grateful to the Alcator C-Mod team for the excellent machine operation, which enabled us to obtain the results discussed here. We also acknowledge many valuable comments of S. Krasheninnikov. This work has been supported by the U.S. Department of Energy Contract No. DE-AC02-02-78ET51013.

Appendix

Using a simple electron thermal conduction model it is possible to interpolate experimental measurements and obtain the plasma temperature as a function of distance along a field line. With two measurements of the plasma temperature on a given field line and an estimate of the heat flux to the divertor plate, the two constants of integration and the volumetric heat source in the conduction equation can be evaluated. Such a calculation has been carried out with Alcator C-Mod data, including radiation losses, by LaBombard [22] and including both radiation loss and momentum loss due to collisions with neutrals by Kesner [47]. In both cases it has been found that the temperature drops only at a very short distance from the target,(poloidally and along a field line) giving a detachment 'front' parallel to the plate. This results in a high ionization rate of neutrals entering the SOL and consequently a low albedo for neutrals (and a low transmission) even at high density. The albedo calculated with this model at high density is too low to explain the particle balance discussed in section 4. An independent argument that the conduction models are inaccurate near the target is that under the predicted conditions for ne and Te, about 50% of the neutrals leaving the target would be ionized. This would result in high currents near the strike point even in detached discharges. Such currents are a factor of 3-10 above those measured experimentally by the probes and thus such a model is inconsistent with the data. The Kesner model also implies that the radiation is very close to the target which is inconsistent with bolometry measurements in the detached divertor state [48].

As a lower bound to the plasma temperature we consider the case where T_e is constant along field lines from the value at the target probe up to the divertor nose. Such a situation could arise if heat transport was predominantly by convection in this region. Above the nose we use values from the Kesner model. Ionization of neutrals in the SOL is consistent with the measured ion currents to the target for this plasma model. The albedo calculated using this model gives an approximately constant ratio of source to sink divertor particle fluxes across the whole plasma density range explored.

References

[1] eg Burt, J., McCracken, G.M., Stott, P.E., Plasma Wall interactions, Proc Int Symp, Ju,lich,FRG 1976, Pergamon Press, Oxford, pg.457

[2] M Keilhacker and K Lackner, J Nucl. Mater. 111-112 (1982) 370.

[3] Shimada, M., Nagami, M., Ioki, K., et al J Nucl. Mater. 111-112 (1982) 362.

[4] De Boo, J.C., Brooks, N.H., DeGrassie, J.S., et al, Nuclear Fusion 22 (1982) 572

[5] Abou-Gabal, H.H. and Emmert, G.A., Nucl. Fusion 31 (1991)407

[6] Dylla,H.F., Bell, M.G., Fonck,R.J., et al J Nucl. Mater. 121 (1984) 144.

[7] Fonck, R.J., Bell ,M.G., Bol, K., et al, J Nucl. Mater,128 - 129 (1984)330.

[8] Lackner, K., Keilhacker, M., J Nucl. Mater,128 - 129 (1984)368.

[9] Stangeby, P.C., Nucl Fusion, 33, (1993) 1695

[10] P Ghendrih et al J Nucl. Mater 220-222 (1995) 307

[11] Janeschitz, G., J Nucl Mater., 220-222, (1995) 73

[12] Kaye, S.M., Bell, M. G., Bol, K., et al., J Nucl Mater., 121, (1984) 115

[13] Heifetz, D.B., Neutral Particle Transport in "Physics of Plasma Wall Interactions in Controlled Fusion", Post , D.E. , Behrisch, R., Eds., Proc of NATO Advanced Study Institute, Val Morin, Quebec, Plenum Press, New York 1986, 695-771

[14] Harrison M.F.A "Atomic and Molecular collisions in the Plasma boundary", in "Physics of Plasma Wall Interactions in Controlled Fusion", Post , D.E. , Behrisch, R., Eds., Proc of NATO Advanced Study Institute, Val Morin, Quebec, Plenum Press, New York 1986, 695-771

[15] Hutchinson, I.H., Boivin, R., Bombarda, F., et al., Phys of Plasmas, **1**, (1994) 1511

[16] Varian Vacuum Products ,Lexington MA ,02173, Ionization gauge type 572,

[17] Niemczewski, A., Lipschultz, B., LaBombard, B. and McCracken, G.M., Rev Sci Instrum , 66, (1994) 360

[18] Haas, G., Gernhardt, J., Kelhacker, M., et al., J Nucl Mater 121 (1984) 151, and US patent No 4792763

[19] Klepper, C.C., et al J Vac. Sci. Technol. 11(1993) 446

[20] Niemczewski, A .P., Doctoral Dissertation, "Neutral Particle Dynamics in the Alcator C-Mod Tokamak" MIT Department of Nuclear Engineering and MIT Plasma Fusion Center Report PFC/RR-95-8, Aug 1995

[21] MKS Instruments Inc., Andover MA 01810 , Baratron Pressure Transducers Type 626 and 131

[22] LaBombard, B., Goetz, J., Kurz, C., et al., Phys of Plasmas, **2**, (1995) 2242

[23] Petrie, T., et al submitted to Nuclear Fusion,(Ms 6023) GA Report GA-A21879, "Radiative divertor experiments in DIII-D with D_2 injection"

[24] Ehrenberg, J K., Campbell, D J., Clement-Lorenzo, S., et al, 22nd European Physical Society Conference on Controlled Fusion and Plasma Physics, Bournemouth, July 1995, Vol **19C** part I pg.309.

[25] Mahdavi , M. A., DeBoo, J.C., Hsieh, C.L., et al. Phys Rev Letters 47 (1981) 1602

[26] Lipschultz, B., Goetz, J.A., LaBombard, B., et al, J. Nucl. Mater., 220-222, (1995) 50

[27] Lipschultz, B., Goetz, J.A., LaBombard, B., et al., European Physical Society Meeting on Plasma Physics Bournemouth, July 1995, Vol 19C part III pg.325.

[28] Klepper C.C. , Hogan J. T., Hill, D. N., et al, Nuclear Fusion 33 (1993) 537.

[29] Maingi, R., Mioduszewski, P.K., Cuthbertson, J.W., et al, J Nucl. Mater 220-222 (1995) 320.

[30] Petrie, T., et al , GA Report GA-A22154

[31] Campbell, D J. and the JET team, Proc 15th IAEA Conf. on Plasma Physics and Controlled Nuclear Fusion Research, paper IAEA-CN60/A-4-I-a , Seville, Spain, Sept 1994.

[32] Hutchinson, I H., Labombard, B., Goetz, J.A., et al, Plasma. Phys and Contr. Fusion, 37 (1995) 1389.

[33] Heifetz, D.B., Petravic, M., Post, D.E., J Nucl. Mater. 121 (1984) 189.

[34] Allen, S. L., Rensink, M. E., Hill, D. N., J Nucl. Mater. 162-164 (1989) 80.

[35] Haas, G., Bachmann, P., Duchs., et al, J Nucl. Mater. 196-198 (1992) 481.

[36] Bachman, P., and Reiter, D., Contrib Plama Phys 35 (1995) 45.

[37] Ruzic, D. N., J Nucl. Mater. 220-222 (1995) 1091.

[38] Stotler, D.P., Snipes, J.A., McCracken, G.M., et al Controlled Nuclear Fusion Research, Modeling of Alcator C-Mod Divertor Plasmas in High Recycling and Detached Regimes .Proc. of the15th International Conference on Plasma Physics, Paper IAEA-CN-60/D-III-1(2)

[39] Janev, R K., Langer, W D., Evans, K. Jr., Post, D E., "Elementary processes in hydrogen-helium plasmas", Springer Verlag, Berlin, 1987

[40] Heifetz, D.B., et al , J Comp. Phys., **46**, (1982) 309

[41] Schultz, D R., Ovchinnikov, S. Yu. and Passovets, S V.," Elastic and Related Cross Sections for Low-Energy Collisions among Hydrogen and Helium Ions, Neutrals, and Isotopes", in "Atomic and Molecular Processes in Fusion Edge Plasmas" (Edited by R.K. Janev, Plenum Press, New York, 1995), p. 279 to be published.

[42] Bachman, P., and Belitz, H J., "Elastic processes in hydrogen-helium plasma: collision data", Max Planck Institut für Plasmaphysik, Report IPP 8/2,1993

[43] Thomas, E W., Janev, R K., and Smith, J., Nucl Instrum and Methods, **B69** (1992)427

[44] Matthews, G F., Fielding, S J., McCracken, G M.,et al., Plasma Phys and Contr. Fus., **32,**(1990) 1301

[45] Stangeby, P C., Pitcher, C S., and Elder, J D., Nucl. Fusion, **32**, (1992) 2079

[46] Gunn, J P., Boucher, C., Stansfield, B L., Savoie, S., Rev. Sci .Instrum., **66**, (1995) 154.

[47] Kesner, J., Phys of Plasma, **2** (1995) 1982.

[48] Goetz, J.A. et al, Phys of Plasma, **2** (1995) to be published.

Figure Captions

Fig. 1 Location of the neutral pressure gauges and the Langmuir probes in the Alcator C-Mod tokamak.

Fig. 2a Time dependence of the neutral pressure in the divertor and at the mid-plane during a strong gas puff (discharge 950309033); The discharge had a lower x-pointwith the outer strike point on the vertical target. The divertor pressure is measured with the capacitance gauge. Detachment occurs at ~0.58 s.

Fig. 2b Effect of a fast divertor detachment (at t=0.86 sec.) and attachment (at t=0.94 sec.) on neutral pressures (discharge 940623015). The divertor neutral pressure is measured with the MIT ionization gauge. The discharge had a lower x-point with the outer strike point on the vertical target; I_p=0.8 MA, $\bar{n}_e = 1.0 \times 10^{20}$ m^{-3}. A detailed description is provided in the main text.

Fig. 3a Mid-plane neutral pressure as a function of core plasma line average density plotted with symbols indicating the edge plasma regimes. The outer strike point is on the vertical target and the divertor pressure is measured with the capacitance gauge.

Fig. 3b Divertor neutral pressure as a function of plasma density. The outer strike point is on the vertical target and the divertor pressure is measured with the capacitance gauge.

Fig. 4 The compression ratio (divertor to mid-plane neutral pressure) dependence on core plasma density, $\bar{n}_e$, showing the SOL plasma transport regimes with different symbols.The outer strike point is on the vertical target and the divertor pressure is measured with the capacitance gauge.

Fig. 5 Dependence of the neutral compression ratio (divertor to mid-plane pressure) on the plasma heating current. The outer strike point is on the vertical target and the divertor pressure is measured with the capacitance gauge.

Fig. 6 Divertor neutral pressure plotted as a function of the distance between the gas-box entrance and the outer strike-point position. The coordinate ρ is the distance of a given flux surface to the separatrix, measured at the tokamak mid-plane.

Fig. 7 Comparison of the divertor neutral compression ratio dependence on density with the strike point on the vertical target plate and on the plate above divertor nose.

Fig 8 Comparison of the divertor neutral compression ratio dependence on density with BxgradB ion drift towards and away from the target plate. The outer strike point is on the vertical target and the divertor pressure is measured with the capacitance gauge.

Fig. 9a Mid-plane pressure plotted as a function of the integrated ion flux striking the target plate above the outer divertor nose. The ion current is measured with divertor domed probes.

Fig. 9b Divertor neutral pressure plotted as a function of the integrated ion flux striking the vertical target plates (inner and outer) below the divertor nose. The outer strike point is on the vertical target and the divertor pressure is measured with the capacitance gauge.

Fig. 10 Simplified picture of particle fluxes that determine the divertor neutral pressure.

Fig. 11 Ratio of the integrated ion flux (measured by the domed probes) at the vertical target plates to the kinetic flux towards the plasma plotted as a function of the core plasma density. The outer strike point is on the vertical target and the divertor pressure is measured with the capacitance gauge.

Fig. 12 Spatial distribution of the chords used during the 1D neutral transport calculations across the divertor plasma fan, The boundary between the PFZ particle reservoir and the plasma is marked by the ρ =-2 mm flux surface. Flux surfaces are shown for discharge 950202013, at 0.68 s.

Fig. 13 Comparison of the source/sink ratio in the divertor neutral flux balance for two different models of the plasma parameters. The balance of the source to the gas kinetic flux directly calculated from the measured neutral density ,(i.e., assuming an albedo A=1), is also shown

Table I: Divertor neutral particle flux balance. The top panel reviews measured and estimated fluxes: vertical plate (inner and outer) ion flux as measured by the domed Langmuir probes, Γ_{plate}, leakage flux ,Γ_{leak}, kinetic flux of neutrals crossing the PFZ-reservoir/plasma boundary, Γ_{kin}, and the source to sink ratio excluding reflection and transmission. The middle and the bottom panels summarize flux balance calculations using the "electron-conduction" and the "constant-T_e" plasma models respectively.

Discharge Number:		6	7	10	11	13
core electron density	[1e20/m3]	1.01	1.26	1.57	1.86	2.09
<u>Measured/estimated fluxes</u>						
Source: Γ_{plate}	[1e22 D^+/s]	0.79	1.60	2.38	0.67	0.66
Sink: Γ_{leak}	[1e22 2*D2/s]	0.11	0.50	1.57	2.06	2.39
Sink: Γ_{kin}	[1e22 D^o/s]	3.08	14.33	44.35	55.86	65.35
$\Gamma_{plate}/\Gamma_{kin}$		0.246	0.108	0.052	0.012	0.010
<u>Electron-conduction plasma model:</u>						
f_{tr}		0.907	0.908	0.807	0.709	0.520
Source: $f_{tr}.\Gamma_{plate}$	[1e22 D^o/s]	0.71	1.46	1.92	0.48	0.34
Albedo; A		0.478	0.660	0.667	0.803	0.776
Sink: (1-A)Γ_{kin}+Γ_{leak}	[1e22 D^o/s]	1.7	5.4	16.3	13.1	17.0
Source/Sink		0.415	0.271	0.117	0.037	0.020
<u>Constant-Te plasma model:</u>						
f	[1]	0.907	0.945	0.912	1.000	1.000
Source: $f_{tr}.\Gamma_{plate}$	[1e22 D0/s]	0.71	1.51	2.17	0.67	0.66
Albedo: A	[1]	0.481	0.729	0.750	0.971	0.975
Sink: (1-A)Γ_{kin}+Γ_{leak}	[1e22 D0/s]	1.7	4.4	12.7	3.7	4.0
Source/Sink		0.417	0.345	0.171	0.183	0.164

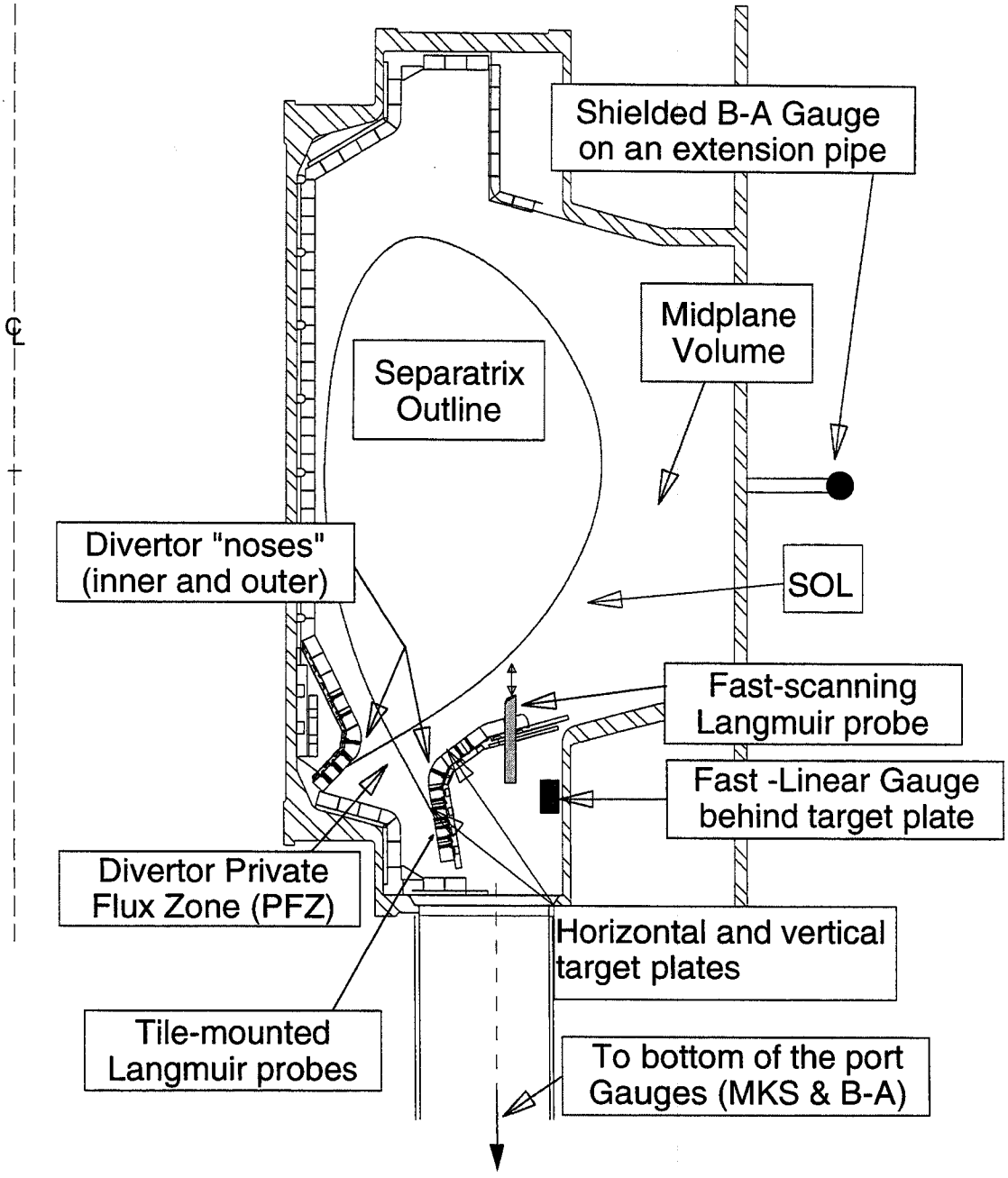
Shielded B-A Gauge
on an extension pipe
Midplane
Volume
Separatrix
Outline
Divertor "noses"
(inner and outer)
SOL
Fast-scanning
Langmuir probe
Fast -Linear Gauge
behind target plate
Divertor Private
Flux Zone (PFZ)
Horizontal and vertical
target plates
Tile-mounted
Langmuir probes
To bottom of the port
Gauges (MKS & B-A)

Fig. 01

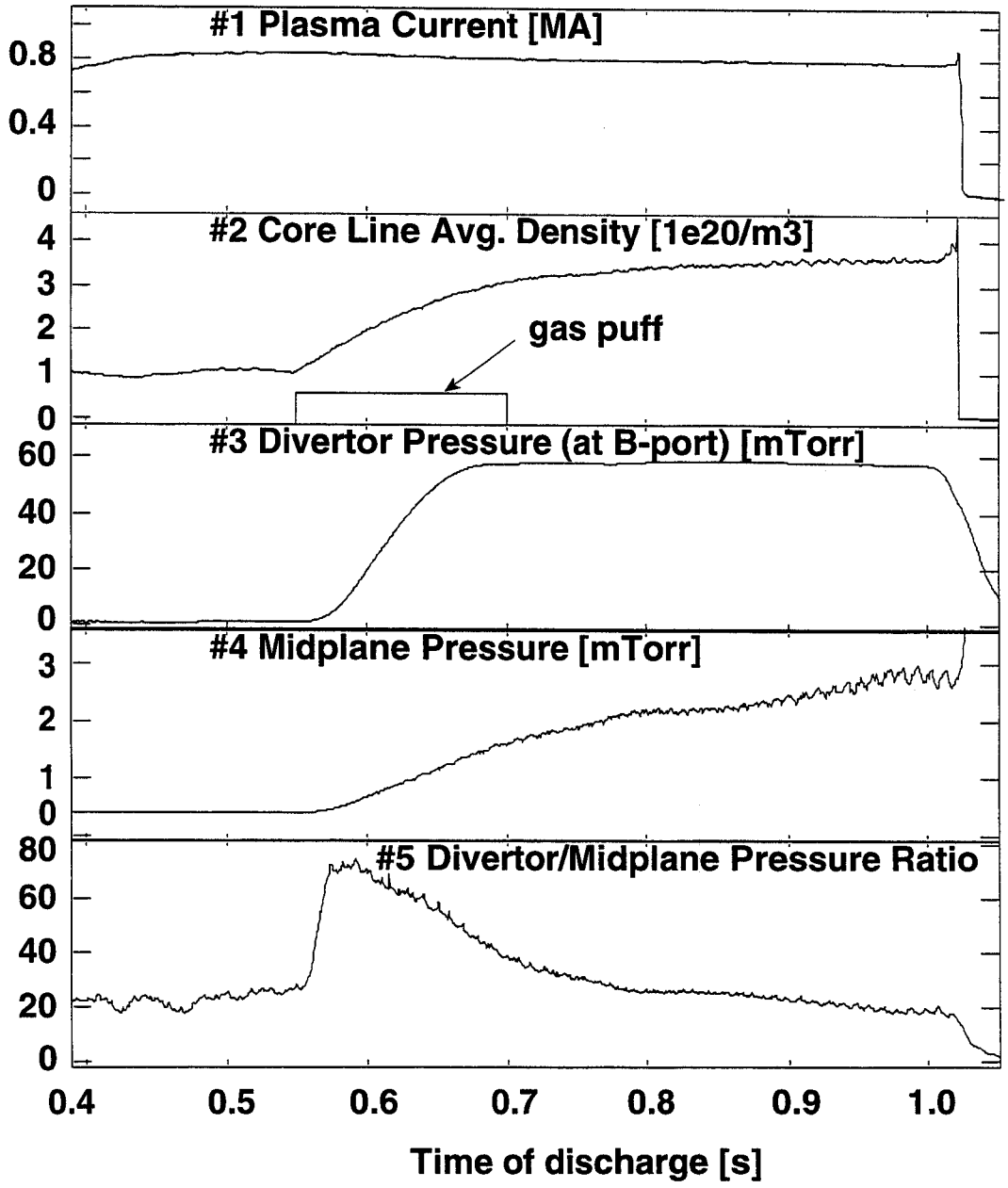
#1 Plasma Current [MA]
0.8
0.4
0
#2 Core Line Avg. Density [1e20/m3]
4
3
2
1
0
gas puff
#3 Divertor Pressure (at B-port) [mTorr]
60
40
20
0
#4 Midplane Pressure [mTorr]
3
2
1
0
#5 Divertor/Midplane Pressure Ratio
80
60
40
20
0
0.4
0.5
0.6
0.7
0.8
0.9
1.0
Time of discharge [s]

Fig. 02a

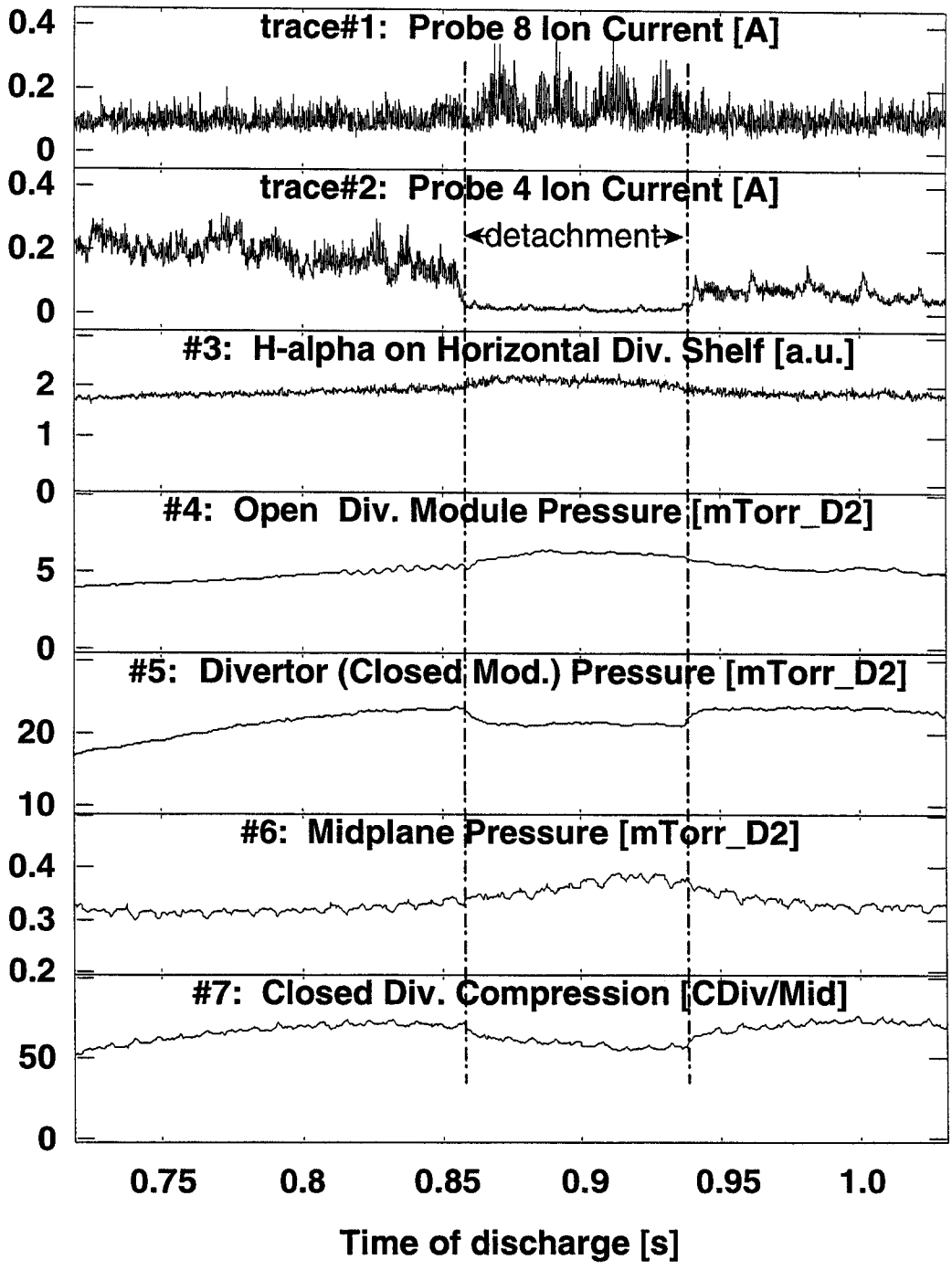
trace#1: Probe 8 Ion Current [A]
0.4
0.2
0
trace#2: Probe 4 Ion Current [A]
detachment
0.4
0.2
0
#3: H-alpha on Horizontal Div. Shelf [a.u.]
2
1
0
#4: Open Div. Module Pressure [mTorr_D2]
5
0
#5: Divertor (Closed Mod.) Pressure [mTorr_D2]
20
10
#6: Midplane Pressure [mTorr_D2]
0.4
0.3
0.2
#7: Closed Div. Compression [CDiv/Mid]
50
0
0.75
0.8
0.85
0.9
0.95
1.0
Time of discharge [s]

Fig. 02b

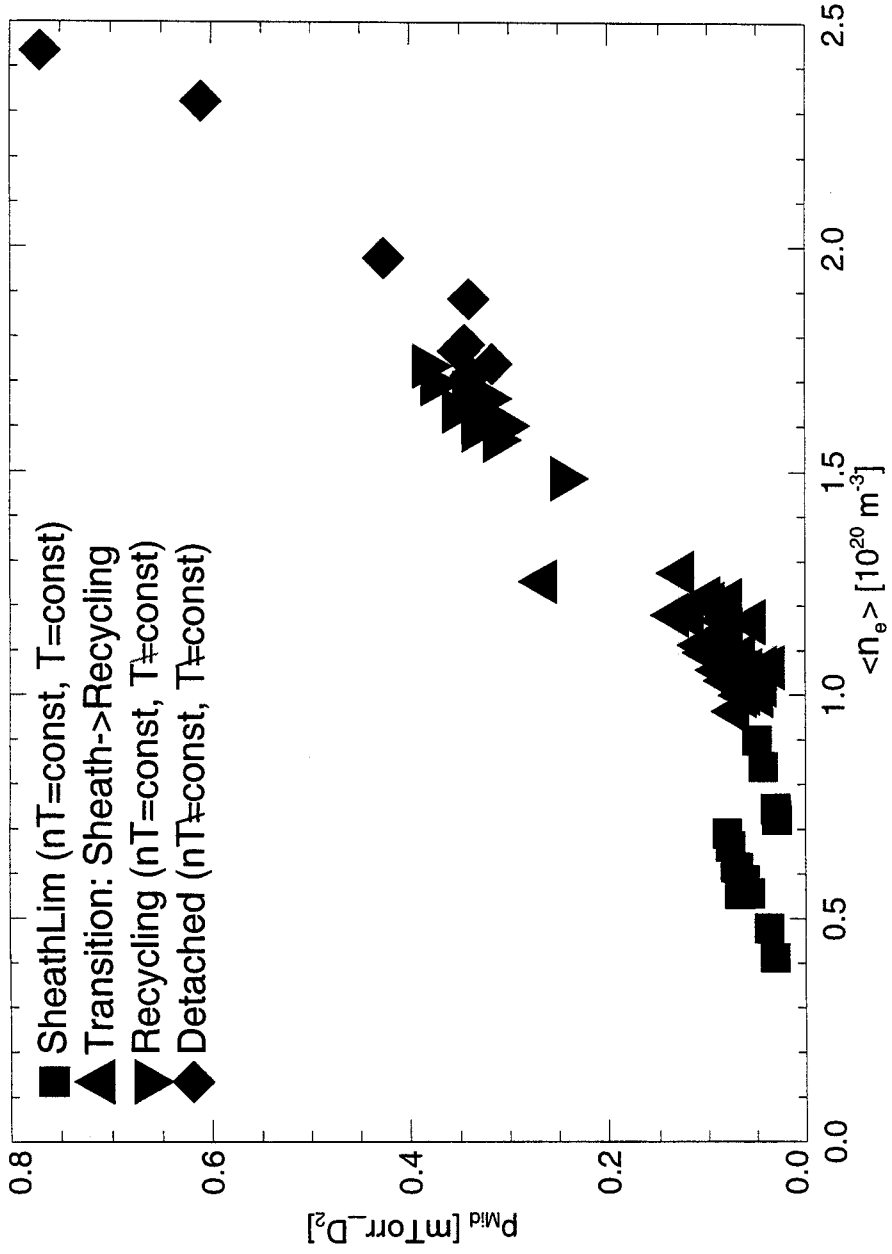
SheathLim (nT=const, T=const)
Transition: Sheath->Recycling
Recycling (nT=const, T≠const)
Detached (nT≠const, T≠const)
p_Mid [mTorr_D2]
<n_e> [10^20 m^-3]
0.0
0.2
0.4
0.6
0.8
0.0
0.5
1.0
1.5
2.0
2.5

Fig. 03a

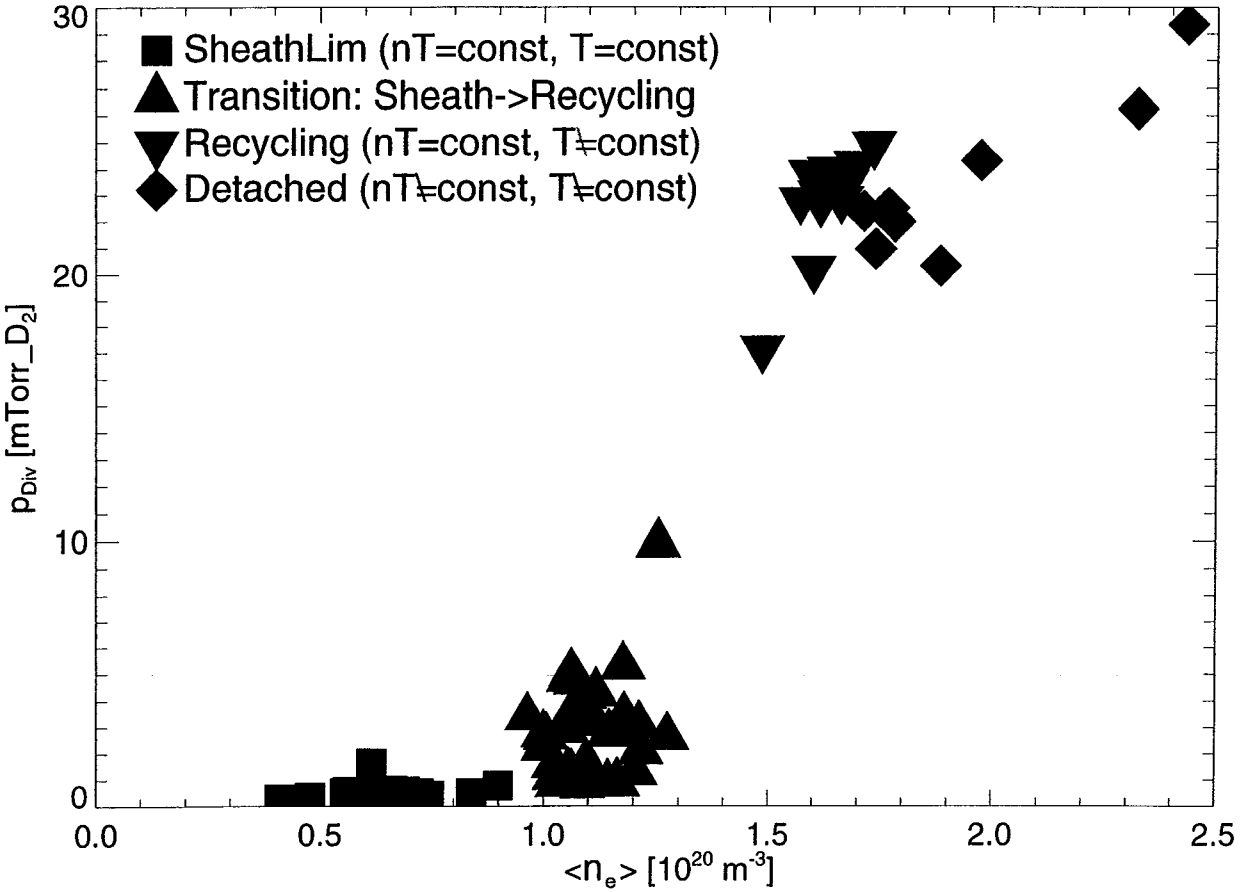
SheathLim (nT=const, T=const)
Transition: Sheath->Recycling
Recycling (nT=const, T≠const)
Detached (nT≠const, T≠const)
p_{Div} [mTorr_D_2]
<n_e> [10^{20} m^{-3}]
0
10
20
30
0.0
0.5
1.0
1.5
2.0
2.5

Fig. 03b

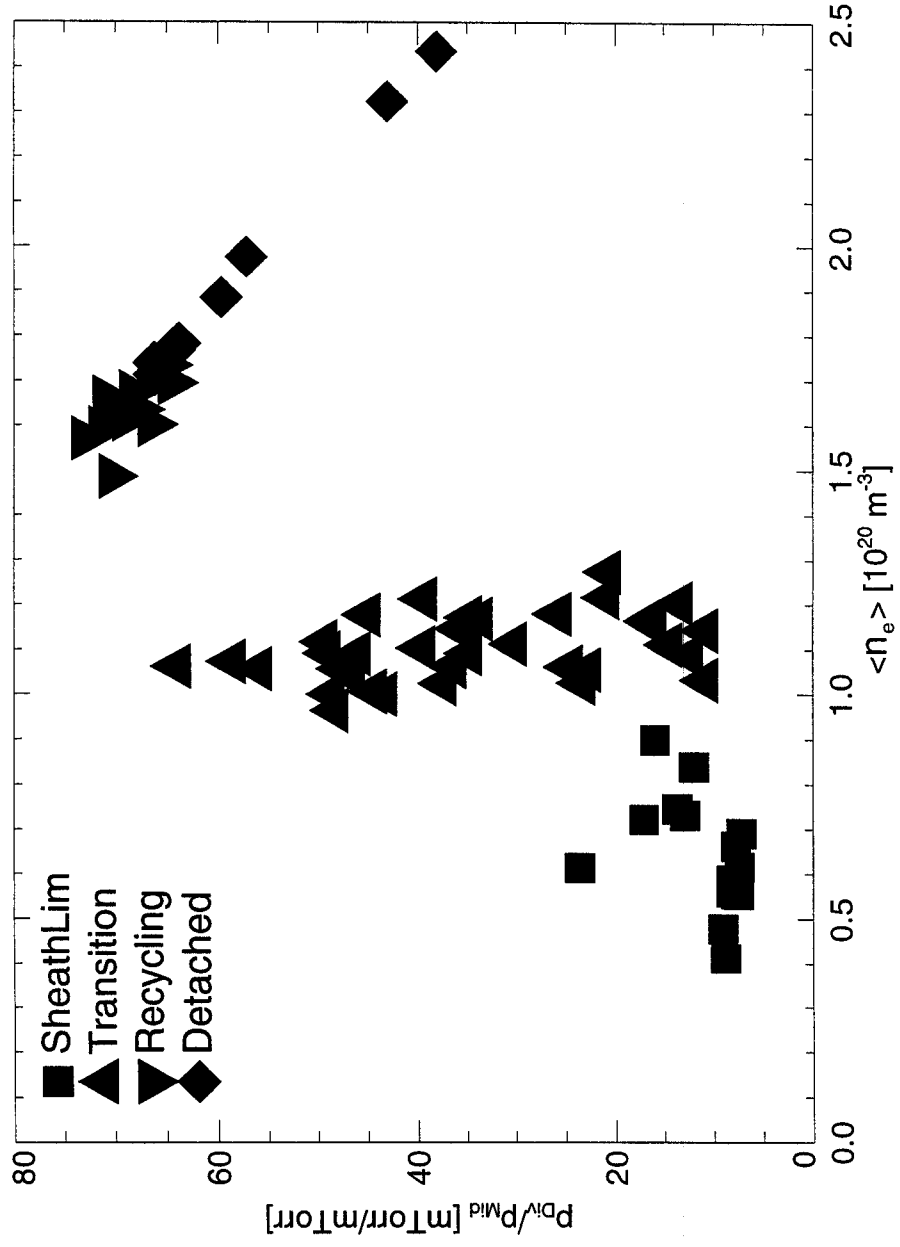
SheathLim
Transition
Recycling
Detached
p_{Div}/p_{Mid} [mTorr/mTorr]
$<n_e>$ [10^{20} m^{-3}]
0
20
40
60
80
0.0
0.5
1.0
1.5
2.0
2.5

Fig. 04

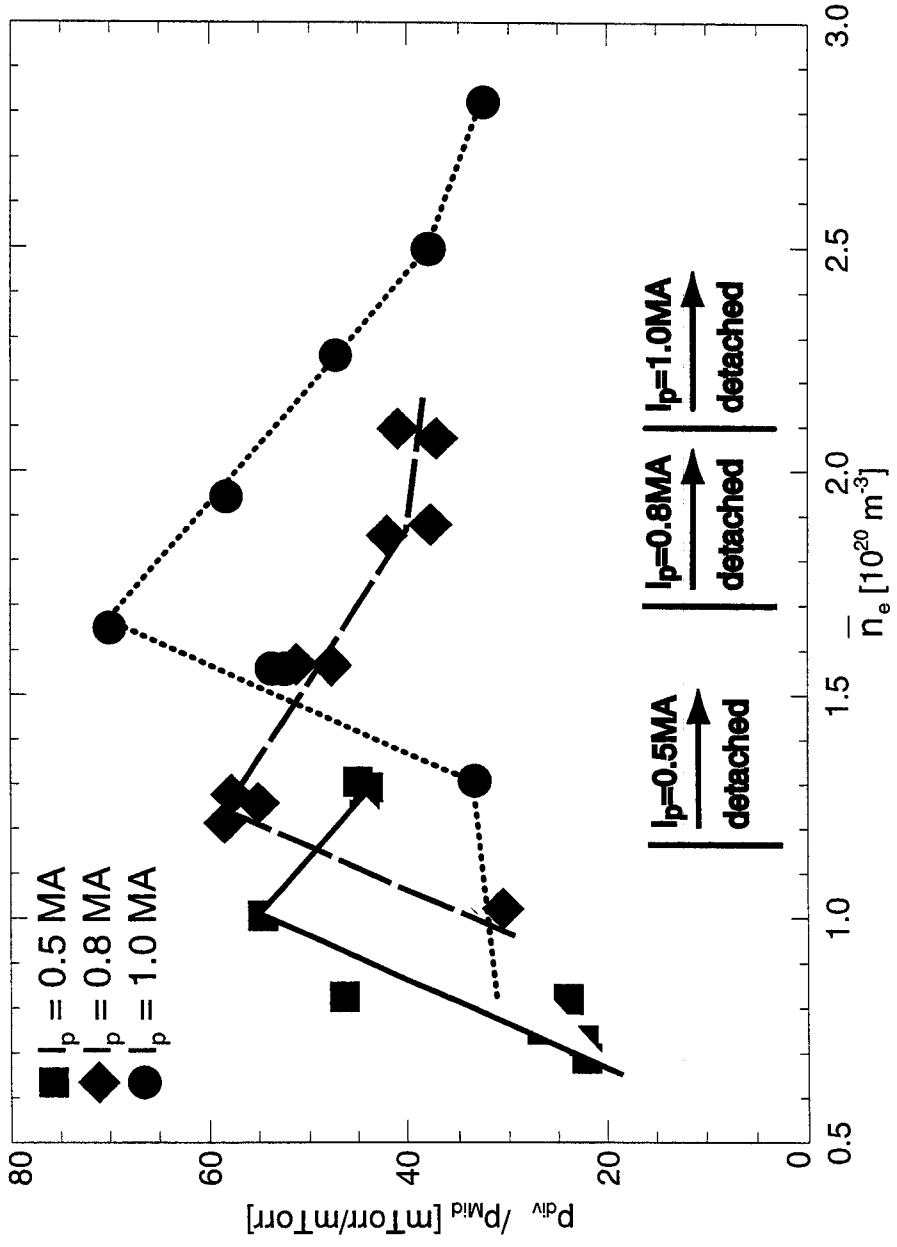
I_p = 0.5 MA
I_p = 0.8 MA
I_p = 1.0 MA
I_p=0.5MA
detached
I_p=0.8MA
detached
I_p=1.0MA
detached
p_{div} /p_{Mid} [mTorr/mTorr]
$\overline{n}_e$ [10^{20} m^{-3}]
0
20
40
60
80
0.5
1.0
1.5
2.0
2.5
3.0

Fig. 05

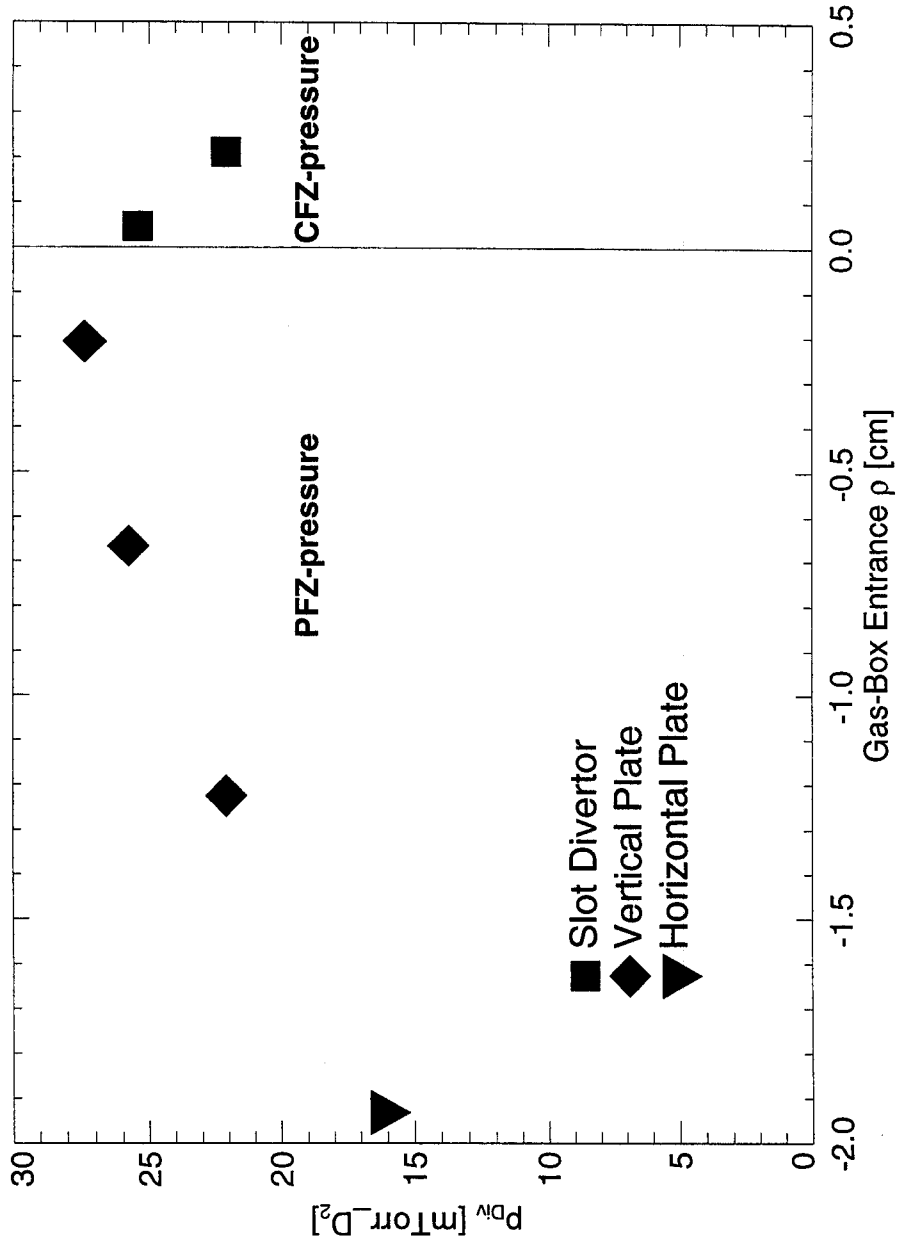
30
25
20
15
10
5
0
-2.0
-1.5
-1.0
-0.5
0.0
0.5
p_{DIV} [mTorr_D_2]
Gas-Box Entrance ρ [cm]
CFZ-pressure
PFZ-pressure
Slot Divertor
Vertical Plate
Horizontal Plate

Fig. 06

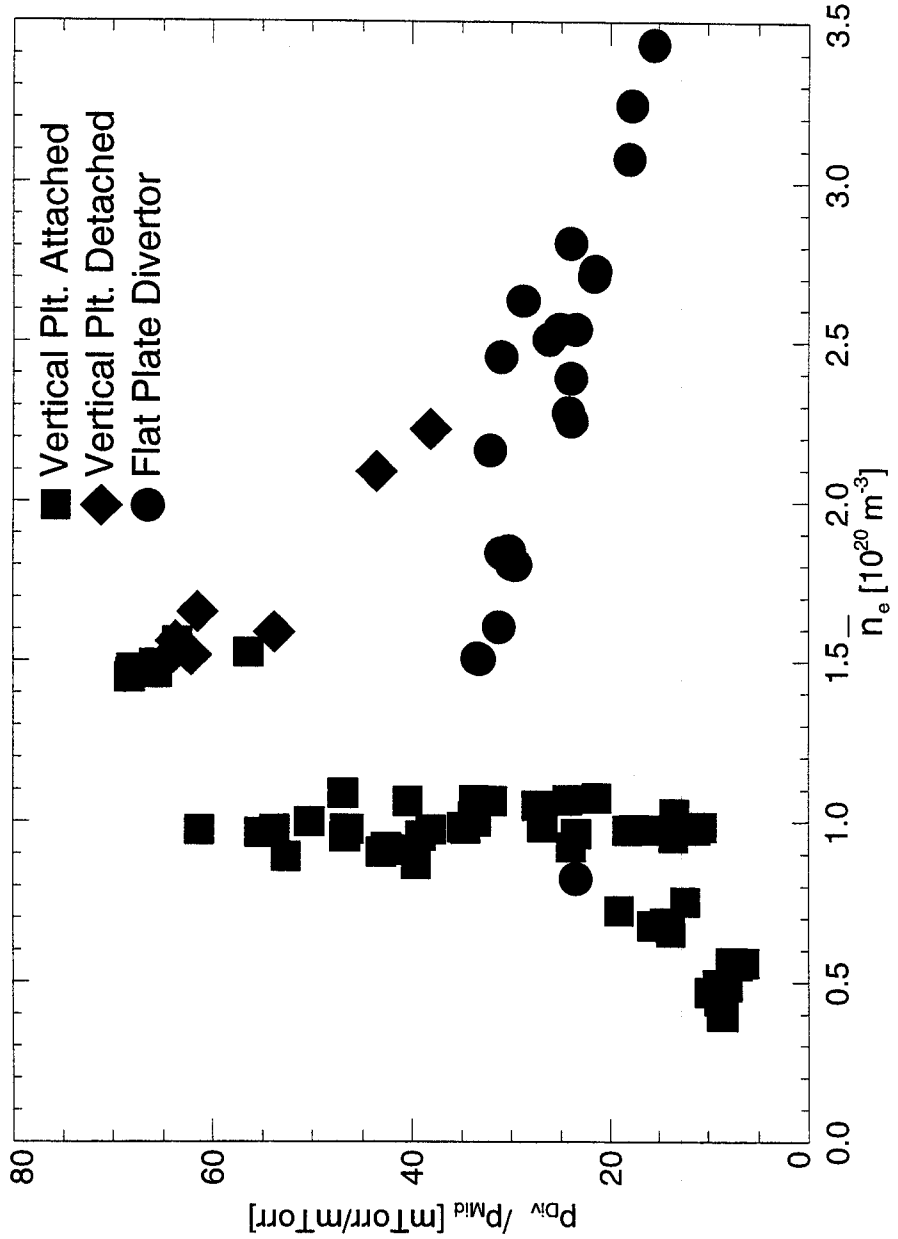
Vertical Plt. Attached
Vertical Plt. Detached
Flat Plate Divertor
p_{Div} /p_{Mid} [mTorr/mTorr]
n_e [10^{20} m^{-3}]
0
20
40
60
80
0.0
0.5
1.0
1.5
2.0
2.5
3.0
3.5

Fig. 07

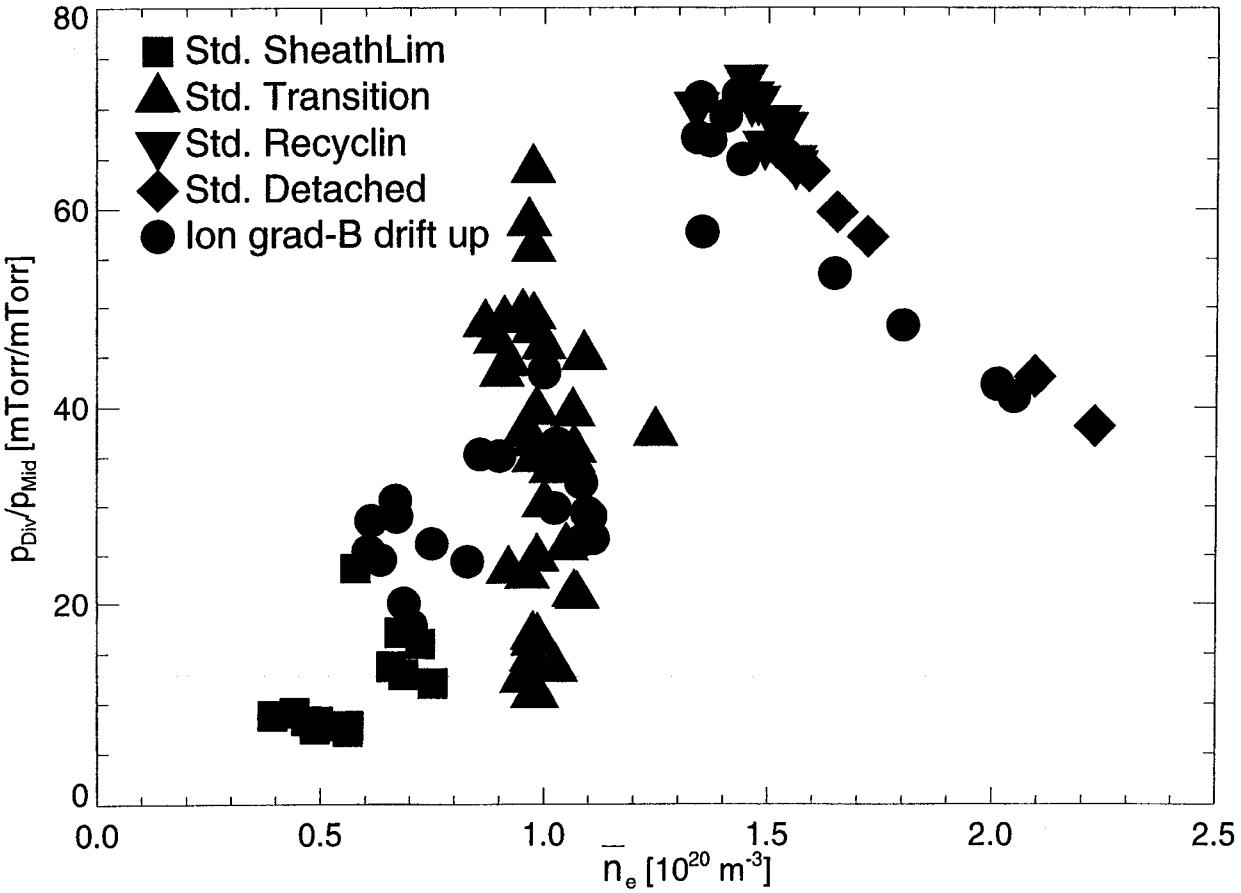
Std. SheathLim
Std. Transition
Std. Recyclin
Std. Detached
Ion grad-B drift up
p_{Div}/p_{Mid} [mTorr/mTorr]
$\bar{n}_e$ [10^{20} m^{-3}]
0
20
40
60
80
0.0
0.5
1.0
1.5
2.0
2.5

Fig. 08

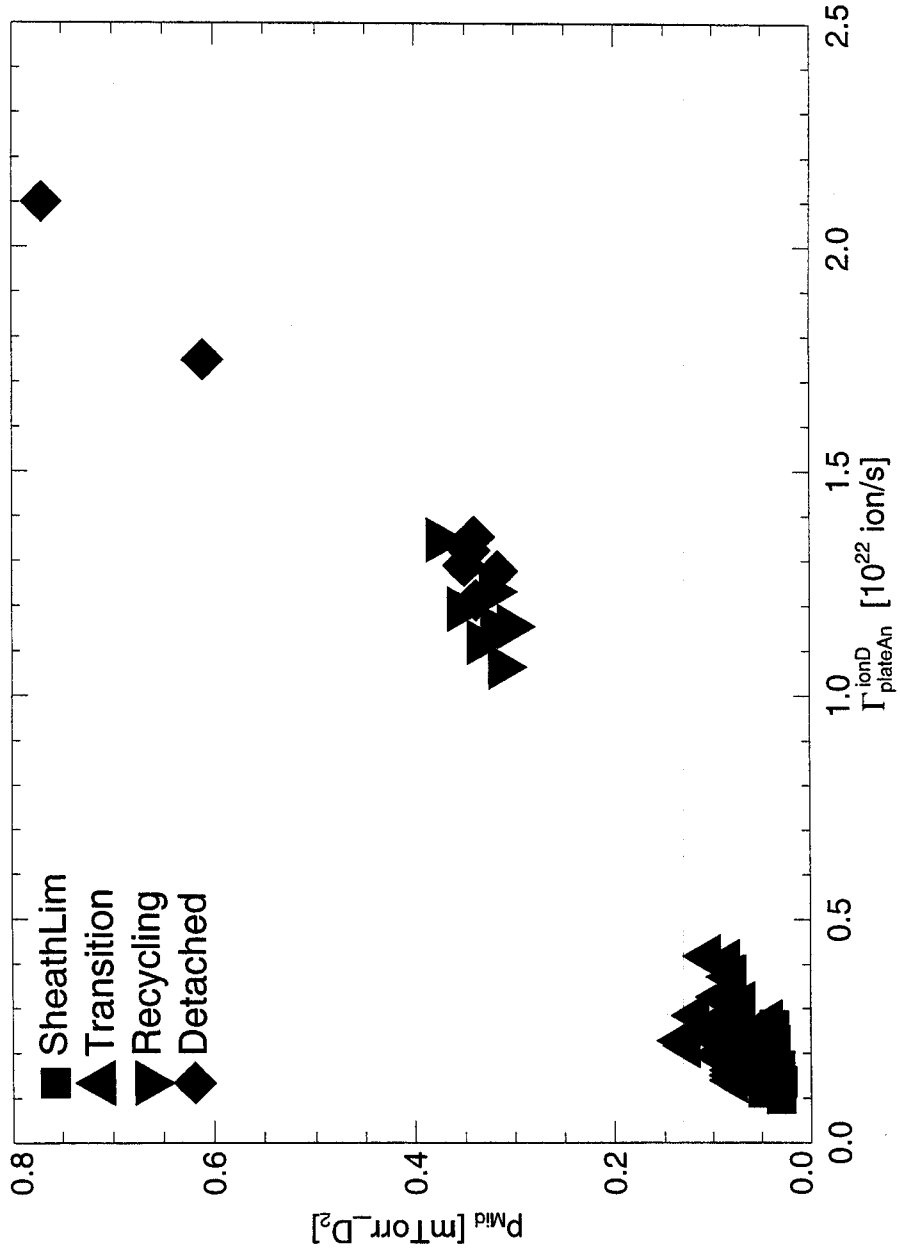
SheathLim
Transition
Recycling
Detached
0.0
0.2
0.4
0.6
0.8
p_{Mid} [mTorr_D$_2$]
0.0
0.5
1.0
1.5
2.0
2.5
$\Gamma^{ionD}_{plateAn}$ [10^{22} ion/s]

Fig. 09a

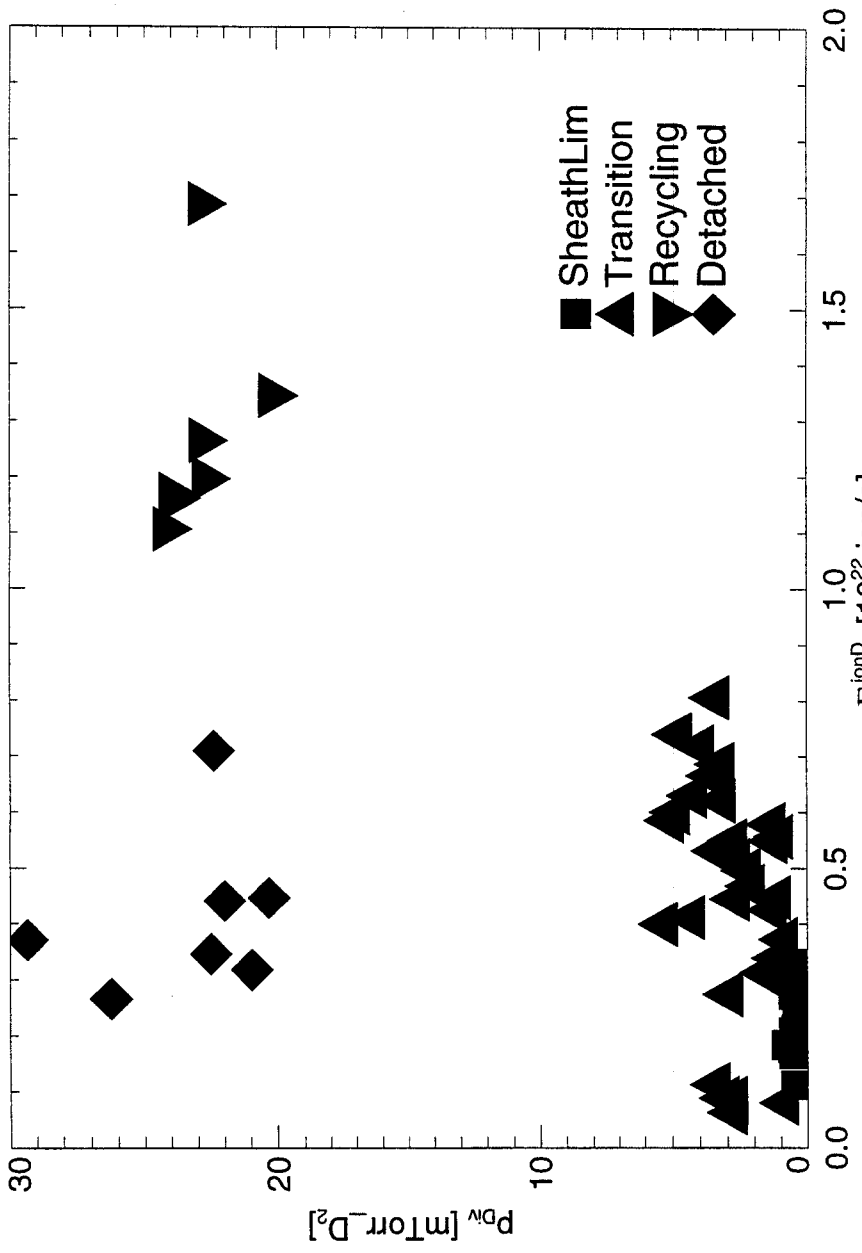
SheathLim
Transition
Recycling
Detached
p_{DIV} [mTorr_D_2]
Γ^{ionD}_{Vplate} [10^{22} ion/s]
0
10
20
30
0.0
0.5
1.0
1.5
2.0

Fig. 09b

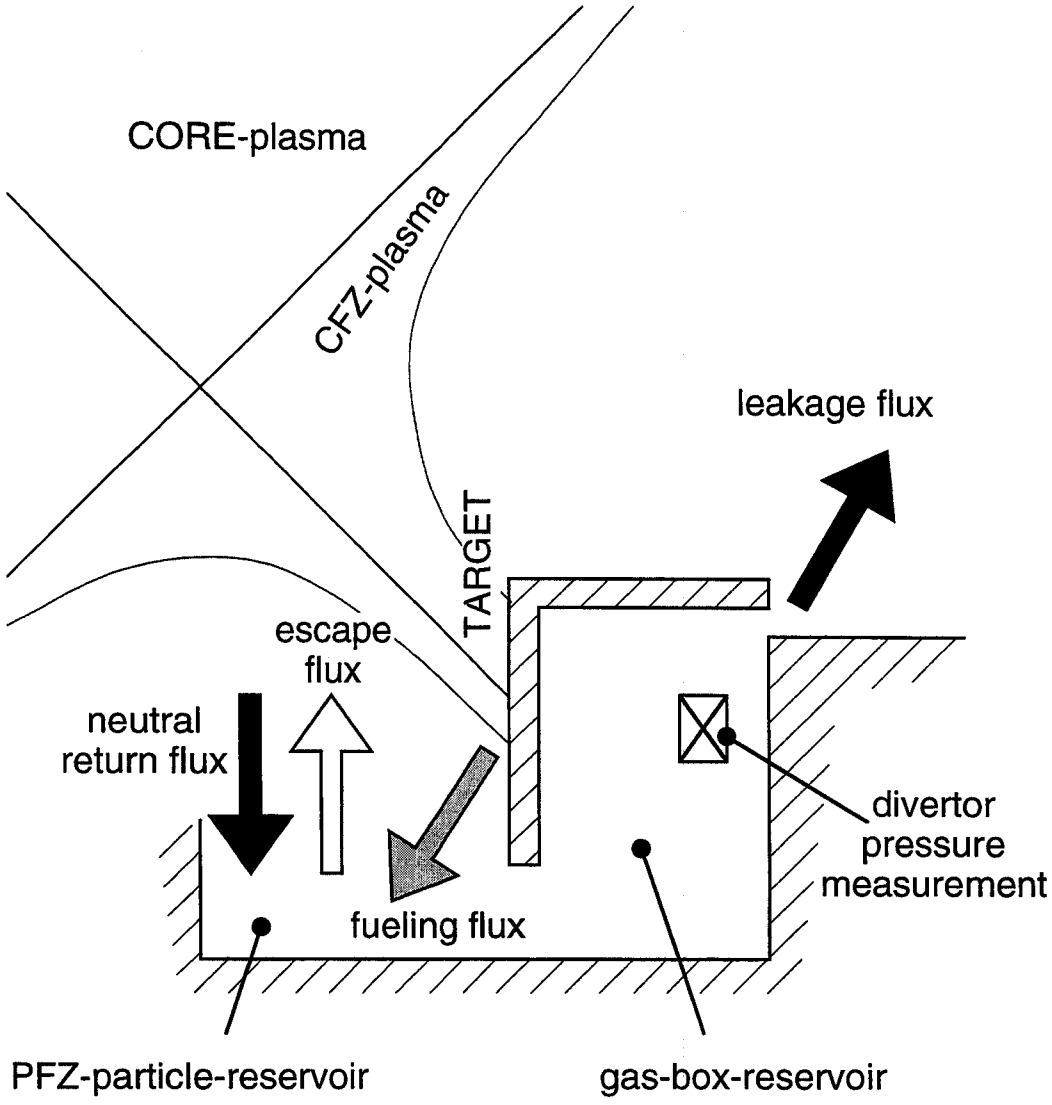
CORE-plasma
CFZ-plasma
leakage flux
TARGET
escape
flux
neutral
return flux
divertor
pressure
measurement
fueling flux
PFZ-particle-reservoir
gas-box-reservoir

Fig. 10

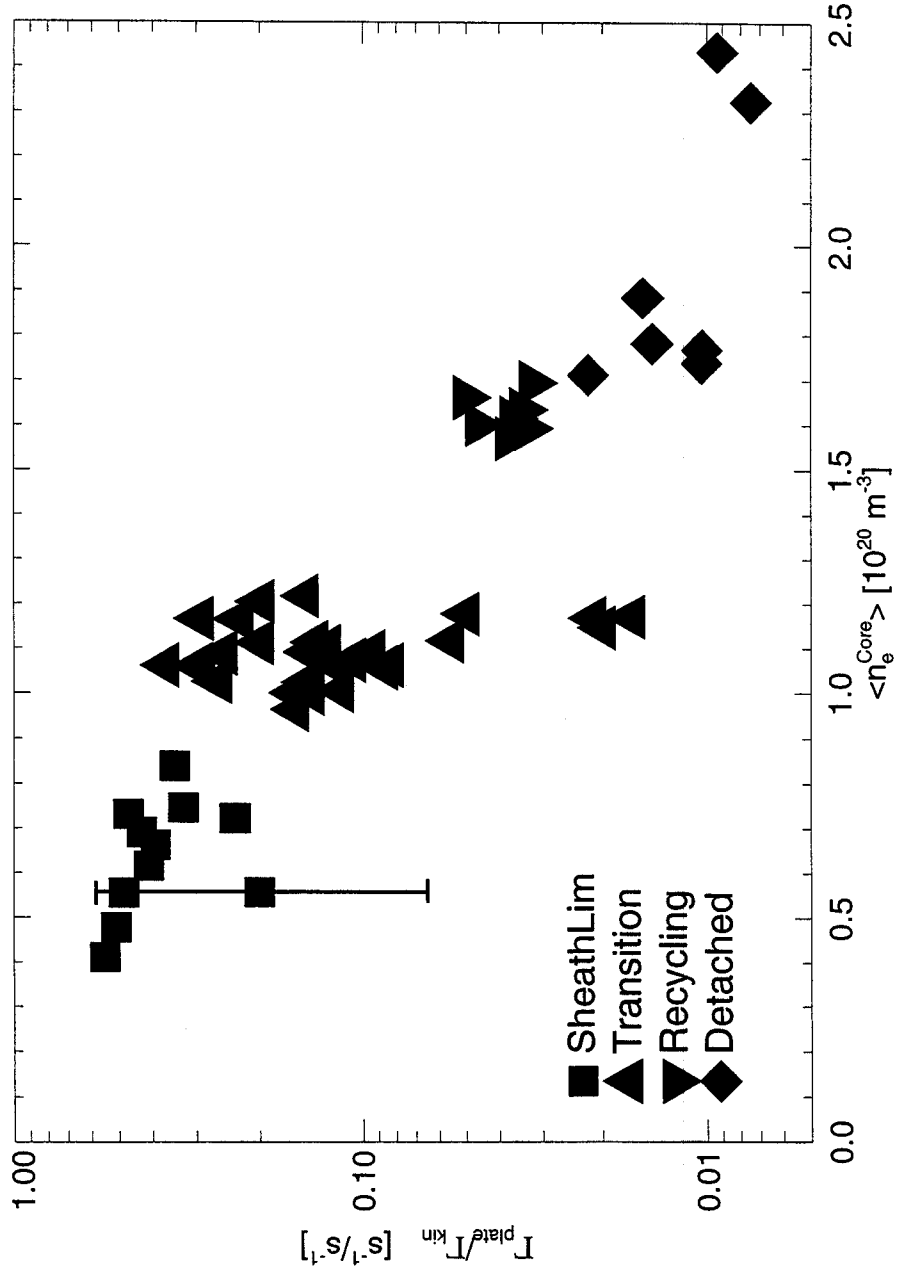
1.00
0.10
0.01
0.0
0.5
1.0
1.5
2.0
2.5
$\Gamma_{plate}/\Gamma_{kin}$ [s^{-1}/s^{-1}]
<n_e^{Core}> [10^{20} m^{-3}]
SheathLim
Transition
Recycling
Detached

Fig. 11

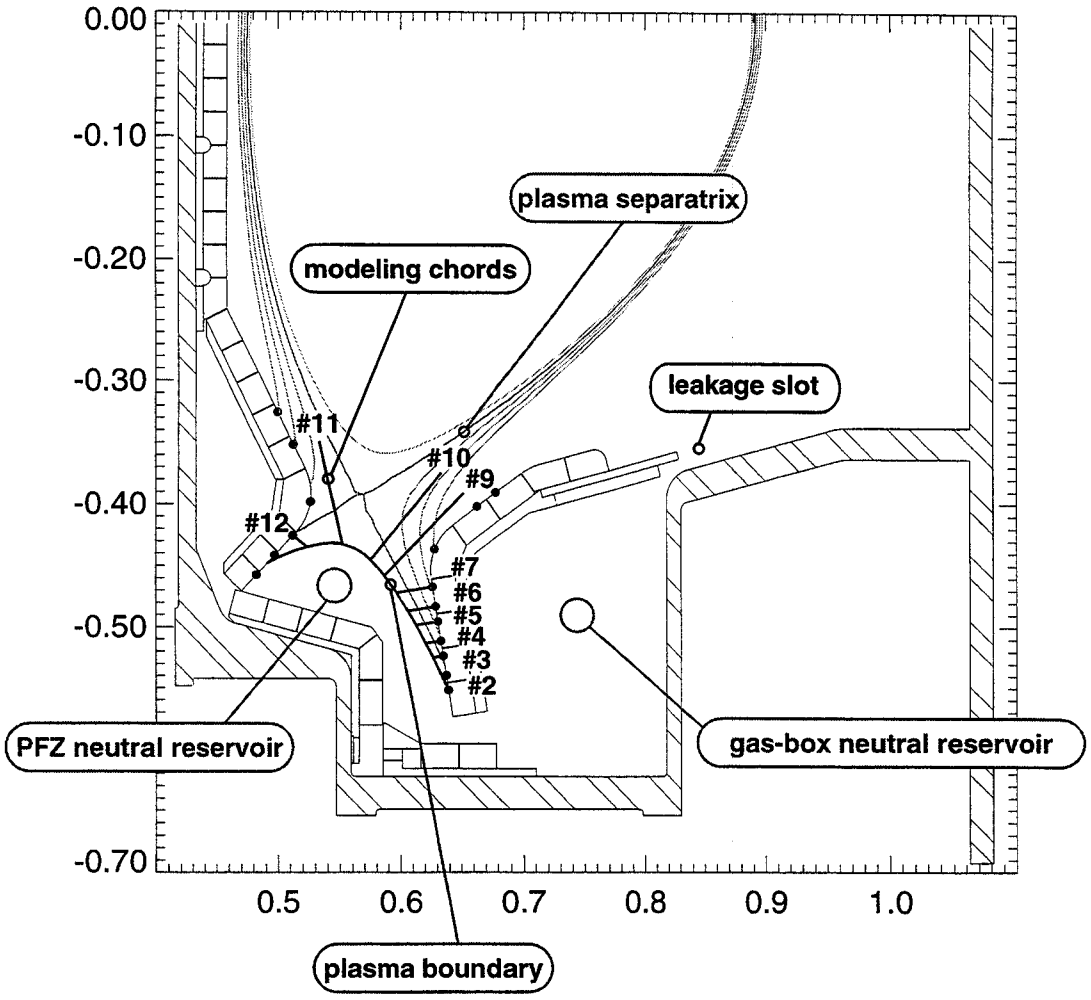
0.00
-0.10
-0.20
-0.30
-0.40
-0.50
-0.70
0.5
0.6
0.7
0.8
0.9
1.0
plasma separatrix
modeling chords
leakage slot
#11
#10
#9
#12
#7
#6
#5
#4
#3
#2
PFZ neutral reservoir
gas-box neutral reservoir
plasma boundary

Fig. 12

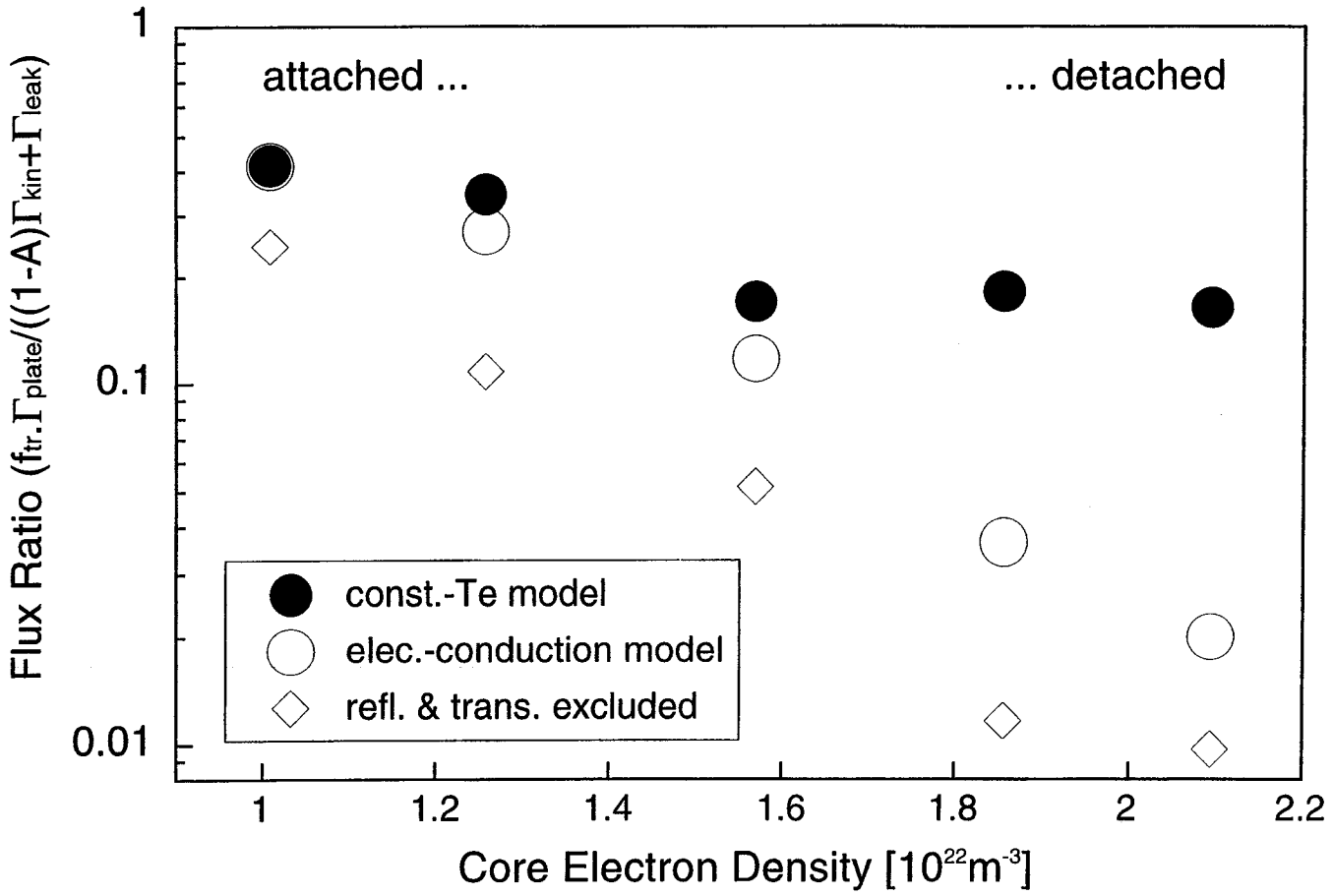
attached ...
... detached
Flux Ratio ($f_{tr}.\Gamma_{plate}/((1-A)\Gamma_{kin}+\Gamma_{leak})$)
1
0.1
0.01
1
1.2
1.4
1.6
1.8
2
2.2
Core Electron Density [$10^{22}m^{-3}$]
const.-Te model
elec.-conduction model
refl. & trans. excluded

Fig. 13